FILE COPY
NO. 1-W

CASE FILE
COPY

NATIONAL ADVISORY COMMITTEE FOR AERONAUTICS

WARTIME REPORT

ORIGINALLY ISSUED
August 1940 as
Advance Confidential Report

HIGH-SPEED DRAG TESTS OF SEVERAL FUSELAGE SHAPES IN COMBINATION WITH A WING

By Eugene C. Draley

Langley Memorial Aeronautical Laboratory
Langley Field, Va.

FILE COPY
To be returned to
the files of the National
Advisory Committee
for Aeronautics
Washington D. C.

NACA

WASHINGTON

NACA WARTIME REPORTS are reprints of papers originally issued to provide rapid distribution of advance research results to an authorized group requiring them for the war effort. They were previously held under a security status but are now unclassified. Some of these reports were not technically edited. All have been reproduced without change in order to expedite general distribution.

HIGH-SPEED DRAG TESTS OF SEVERAL FUSELAGE SHAPES IN COMBINATION WITH A WING

By Eugene C. Draley

L-542

SUMMARY

Drag tests were made in the 8-foot high-speed wind tunnel of 23 conditions combining six streamline shapes and three conventional cowling-fuselage bodies. All the models were tested in combination with a wing in order to include wing-fuselage interference effects. The data were obtained at speeds up to 440 miles per hour, corresponding to a Mach number of 0.60 and to a Reynolds number, based on a representative fuselage length (60 in.), of 17,400,000. Tests were made with both normal and fixed transition; the fixed transition is considered to represent the true drag characteristics at full-scale flight conditions better than normal transition.

The results from the tests of the combinations with three streamline bodies gave effective fuselage-drag coefficients from 0.046 to 0.057 at speeds from 260 to 440 miles per hour. The relative drag of two of these bodies, differing only in fineness ratio, was considerably changed by compressibility effects at high speeds. Relatively blunt noses on streamline bodies in conjunction with the wing produced little or no changes in either the drag or the compressibility effects. A cooling-air intake opening in the blunt nose caused about 7-percent increase in the drag with no significant changes in the compressibility effects. The best radial-engine cowling-fuselage combinations had, without cooling air, drags 18 to 21 percent greater than the corresponding streamline fuselages, depending on the speed and the body.

The critical speeds of the combinations tested were, in general, determined by the wing-fuselage juncture. Calculations indicate that material gains in critical speed would be obtained for the streamline bodies with a wing having a lower peak local velocity than that of the test wing.

INTRODUCTION

Though a considerable amount of aerodynamic data for fuselage shapes is already available, most of these data

are of limited value because of the low Reynolds numbers and particularly of the low Mach numbers of the tests. Present and prospective speeds of aircraft demonstrate the need for data applicable at high speeds where compressibility effects are important.

Investigations of compressibility effects conducted by the NACA have now been extended to include tests of several streamline forms and some modifications of these forms to represent bodies with engines installed.

So far as is known, these data are the first available at such high Mach numbers; compressibility effects up to rather high though, in general, subcritical speeds are included.

APPARATUS AND METHODS

The investigation was conducted in the 8-foot high-speed wind tunnel, a single-return closed-throat type with a circular cross section. The wing of the model completely spanned the test section. Airfoil transition data obtained in this tunnel indicate that the degree of turbulence is low, though greater than that of free air.

In order to include interference effects, the various fuselage-shape combinations were tested in a midwing position on the model of a transport airplane wing used for the tests of reference 1. This wing has a rectangular center section of NACA 2215 airfoil profile; the chord of the center section is 20.25 inches and its span is 35.50 inches. Outboard of the center section, the wing tapers to an NACA 2212 airfoil profile at a station 50.58 inches from the center line of the wing.

Six streamline fuselages (fig. 1) were tested. These models consisted of three streamline bodies with four nose variations. Body 1 with nose 1 is a slight modification of the NACA streamline form 111 (reference 2), giving a fineness ratio of 5.12. Nose 2 was made by foreshortening the axial ordinates of nose 1; the fineness ratio of this nose with body 1 is thus 4.84. Body 2 was made from body 1 by cutting the center section down to a cylindrical shape of a smaller diameter and fairing the ends of this section, which with nose 1 has a fineness ratio of 6.06. Body 2 with nose 2 (fig. 2) has a fineness ratio of 5.23. Nose 2-A (fig. 3) was made by cutting an opening in nose 2

to simulate a cooling-air intake. Body 3 with nose 3 was reproduced from scaled-down ordinates of body 1 with nose 1. The maximum diameter and the fineness ratio are the same as for body 2 with nose 1.

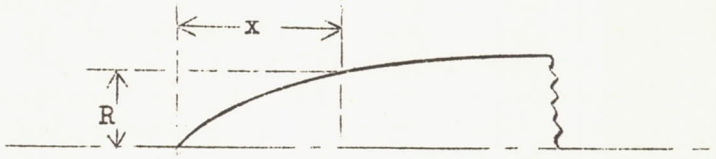
The ordinates for three of the streamline shapes are given in table I. The ordinates for the other shapes can be obtained by combining the ordinates for a particular nose and for a particular body. The dimensions of the nose opening are given in figure 1.

The three radial-engine cowlings tested (fig. 1) have the same shape and designation as in reference 3. Cowling 5 has a sharp leading-edge curvature and a large intake opening. Cowling 7 has a shorter axial length, a smaller intake opening, and a more generous curvature than cowling 5. Cowling C (fig. 4), designed for high critical speed, has the same axial length as cowling 5 but a smaller intake opening.

All cowlings were tested with baffles to provide a suitable pressure drop for engine cooling. A short skirt was used when the cowling exit was open; a long skirt, with slot filled and faired with plasticine, was used when the cowling exit was closed. The dimensions of the combinations with cowlings are included in figure 1. A detailed description of the cowlings, the skirts, and the baffles is given in reference 3.

Great care was taken in the construction and the finishing of the models to insure surface smoothness and accuracy of shape.

TABLE I. Ordinates for Three Fuselage Shapes



Body 1, nose 1		Body 2, nose 2		Body 3, nose 3	
x (in.)	R (in.)	x (in.)	R (in.)	x (in.)	R (in.)
-0.11	0	-	-	-0.11	0
.79	1.28	3.29	0	.79	1.08
1.58	1.93	5.34	2.98	1.58	1.63
3.15	2.89	7.40	4.23	3.15	2.44
6.30	4.14	9.45	4.93	6.30	3.50
[a]9.66	[a]4.98	[a]9.66	[a]4.98	[a]9.66	[a]4.21
12.60	5.46	12.60	5.20	12.60	4.62
18.90	6.03	18.90	5.20	18.90	5.10
24.46	6.15	24.46	5.20	24.46	5.20
31.50	5.97	31.50	5.05	31.50	5.05
37.80	5.46	37.80	4.62	37.80	4.62
44.10	4.52	44.10	3.82	44.10	3.82
50.40	3.16	50.40	2.67	50.40	2.67
53.55	2.42	53.55	2.05	53.55	2.05
56.70	1.63	56.70	1.38	56.70	1.38
59.85	.82	59.85	.70	59.85	.70
61.42	.42	61.42	.35	61.42	.35
63.00	0	63.00	0	63.00	0

[a]Juncture of body and nose. Radial ordinates here are only approximate.

For each of the streamline fuselages, tests were made with normal transition and with transition fixed by means of a thread of 0.01-inch diameter fastened around the nose with shellac. (See fig. 2.) Transition was fixed at approximately the same place as it would occur under full-scale conditions: 4 inches back of the nose tip with the exception of nose 2-A, on which the thread was located at the same place on the surface as for nose 2. For cowling

C, closed, on body 1, the thread was located 0.5 inch back of the leading edge of the cowling. (See fig. 4.) All other cowling-fuselage combinations were tested only with normal transition. The drag of the thread alone was believed to be insignificant. The method and the significance of fixing transition are discussed in reference 1.

The main limitation of the lift and the speed range of the tests was the strength of the models. The range limits and test conditions of this investigation are given in tables II and III.

TABLE II. Limits of Speed Range and Lift Coefficient

Approximate C_L	Fuselage angle of attack, α_F (deg)	Air speed, V (mph)	Mach number, M	Reynolds number, R, based on fuselage length
0.4	2	260	0.35	11,700,000
.3	1	380	.51	15,400,000
.2	0	440	.60	17,400,000
.1	-1	440	.60	17,400,000

TABLE III. Test Conditions

Condition	Combination		Transition	Cowling	Cowling condition	
	Body	Nose			Baffle	Exit
1	1	1	Normal	-	-	-
2	1	1	Fixed	-	-	-
3	1	2	Normal	-	-	-
4	1	2	Fixed	-	-	-
5	1	-	Normal	C	Open	Open
6	1	-	do.	C	Closed	do.
7	1	-	do.	C	do.	Closed
8	1	-	Fixed	C	do.	do.
9	1	-	Normal	5	Open	Open
10	1	-	do.	5	Closed	Closed
11	2	1	do.	-	-	-
12	2	1	Fixed	-	-	-
13	2	2	Normal	-	-	-
14	2	2	Fixed	-	-	-
15	2	-	Normal	C	Open	Open
16	2	-	do.	C	Closed	do.
17	2	-	do.	C	do.	Closed
18	2	-	do.	7	Open	Open
19	2	-	do.	7	Closed	Closed
20	2	2-A	do.	-	-	-
21	2	2-A	Fixed	-	-	-
22	3	3	Normal	-	-	-
23	3	3	Fixed	-	-	-

The angle of attack ranged from -1° to 2° with a speed range from 140 to about 440 miles per hour. The corresponding Mach numbers were from 0.17 to 0.60, and the Reynolds numbers, based on fuselage length, were from 6,500,000 to 17,400,000.

SYMBOLS

The definitions of the symbols used in this report are presented in the following list:

L representative fuselage length

ρ mass density of the air

L-542

V	air speed
q	dynamic pressure $(\frac{1}{2} \rho V^2)$
α_F	fuselage angle of attack
A	maximum cross-sectional area of the fuselage
D_F	effective fuselage drag [(drag of wing and fuselage together - (drag of the wing alone)]
C_{D_F}	effective fuselage drag coefficient (D_F/qA)
C_L	lift coefficient
μ	coefficient of viscosity of air
M	Mach number (the ratio of air speed to the speed of sound in air)
M_{cr}	Mach number at which local speed of sound is reached
R	Reynolds number $(\rho V L/\mu)$

RESULTS AND DISCUSSION

Results for the streamline shapes with fixed transition are presented in figures 5, 6, and 7 together with some results for various radial-engine cowling-fuselage combinations. The more important data in the three figures are plotted against α_F in figure 8. The results for normal transition on streamline bodies are presented in figures 9, 10, and 11 with results for the radial-engine cowling-fuselage combinations.

Table IV includes the more important results of the streamline fuselages with fixed transition and of the cowling-fuselage combinations.

TABLE IV

Condition	Combination	C_{D_F}	
		M = 0.35	M = 0.60
2	Body 1, nose 1	0.0471	0.0512
4	Body 1, nose 2	.0462	.0500
7	Cowling C closed, body 1	.0540	.0570
8	Cowling C closed, body 1 (fixed transition)	.0555	.0587
10	Cowling 5 closed, body 1	.2450	.2820
12	Body 2, nose 1	.0535	.0568
14	Body 2, nose 2	.0526	.0545
17	Cowling C closed, body 2	.0640	.0685
19	Cowling 7 closed, body 2	.0640	[a].1100
21	Body 2, nose 2-A	.0559	.0592
23	Body 3, nose 3	.0517	.0512

[a]This value is approximate.

Comparisons throughout the report are, in general, made on the basis of the fixed-transition data. This procedure is adopted because these data represent more nearly full-scale conditions by approximating full-scale boundary-layer conditions. An exception to this general procedure occurs for the models with cowlings. For these data normal transition is generally well forward, approximating full-scale conditions because the large adverse pressure gradients occurring close to the nose tend to determine the transition location. Any decisive movement of transition on the radial-engine cowlings at Reynolds numbers higher than the ones obtained in these tests is unlikely. As a verification of this procedure, cowling C was tested with both normal and fixed transition. Because of the nature of the pressure distribution for this cowl-

L-542

ing, the greatest transition movements would occur with it. The difference between the normal and the fixed transition data, however, was only 3 percent, which is well within the accuracy required for comparisons of the data. For the other cowlings the difference would be much less.

Streamline shapes.- At low speeds (M = 0.35 or about 260 mph) the C_{D_F} of body 2, nose 1 was 14 percent greater than that of body 1, nose 1 (fig. 5). The actual drag was 19 percent less. This result is partly accounted for by the fact that the surface area of body 2, nose 1 is 12 percent less than that of body 1, nose 1. The higher C_{D_F} for body 2, nose 1 is due to the smaller cross-sectional area, the area used in determining the C_{D_F} values. The C_{D_F} of body 3, nose 3 was about 3.4 percent less than that of body 2, nose 1; body 3, nose 3 had about 3.7 percent less surface area than body 2, nose 1. Thus, at the lower speeds, body 1, nose 1 had the lowest drag coefficient of the three shapes just discussed; body 3, nose 3 and body 2, nose 1 had drag coefficients 10 and 14 percent greater, respectively.

At higher speeds (M = 0.60) there was little difference between body 1, nose 1 and body 3, nose 3. The C_{D_F} of body 2, nose 1, however, was about 11 percent greater than the corresponding values for either of the other two combinations.

In figures 6 and 7, comparisons of the slopes of the estimated incompressible-flow curves and of the experimental curves for body 1, nose 1 and body 3, nose 3, respectively, indicate the probable magnitude of the compressibility effects. The estimated turbulent skin-friction drag data with allowance for fineness-ratio differences for body 1, nose 1, and body 3, nose 3, (figs. 6 and 7) were taken from reference 2. It was assumed that the drag data from this source were all due to turbulent skin friction for Reynolds numbers from 6,000,000 to 20,000,000 and, because of the low speeds at which the data were obtained, the compressibility effects can be considered insignificant. Thus, the difference between the slopes of this estimated curve and the slopes of the fixed-transition data presented in this report indicates the probable magnitude of the compressibility effects.

Body 3, nose 3 had only a small increase in C_{D_F} due to compressibility; whereas, body 1, nose 1 had more serious effects, as might be expected on account of the difference of fineness ratios. The results of the tests of body 2, nose 1 also showed compressibility effects similar to those for body 1, nose 1. These changes of effective drag coefficient with speed were undoubtedly compressibility effects and are illustrative of the errors involved in applying data obtained at relatively low speeds to high speeds where compressibility effects are important. In the consideration of these compressibility effects, it should be appreciated that they are dependent in large measure on conditions at the wing-fuselage juncture. Actually, the critical speed was determined by the aerodynamic interference effects at the wing-fuselage juncture in all cases except for cowlings 5 and 7. These effects will later be discussed in detail.

The two remaining variations in the streamline fuselages were made by the substitution of nose 2, a more blunt nose, for nose 1 on bodies 1 and 2.

At values for M of 0.35 and 0.60, body 1 had a C_{D_F} about 2.3 percent lower with nose 2 than it had with nose 1 (fig. 5). The corresponding decrease in surface area was 3.7 percent.

The similar compressibility effects noted for these two body-nose combinations indicate no change in critical speed. For the bodies alone this conclusion would probably be invalid. In this instance, however, it is likely that the increase in the induced velocity caused by the curvature of the blunt nose exists over only the forward portion of the body and is of smaller magnitude than the maximum induced velocity at the wing-fuselage juncture. The critical speed, as previously noted, is then determined largely by the aerodynamic interference effects at the wing-body juncture.

At low speeds (M = 0.35), the effects of changing the nose shape on body 2 were similar to those on body 1. At higher speeds (M = 0.60), as indicated by the slopes of the corresponding curves in figure 7, the wing-body 2 combination with nose 2 had smaller compressibility effects than did the same combination with nose 1.

A probable reason for the difference is that nose 2, the blunter nose, changed the shape of the velocity distribution over the body. For the body alone, it would normally be expected that nose 2 would have higher local velocities than nose 1 and thus have greater compressibility effects. The region of high local velocity for nose 2, however, probably occurs relatively farther forward on the body and, provided that the peak local velocity was not extremely great, this forward position would tend to give lower induced velocities farther back on the body in the region of the wing-fuselage juncture. Thus, if the maximum local velocity for the body alone is not extremely great, as previously noted, the compressibility effects are in a large measure the result of aerodynamic interference effects at the wing-body juncture. The probable slightly lower local velocities at the wing-body juncture for nose 2 would lead to later critical speed and therefore to smaller compressibility effects for this combination.

A modification, nose 2-A, was made to nose 2 in which an air-intake nose opening was simulated. The nose opening was tested to give some indication of the relative form drag of this shape as compared with that of the radial-engine cowlings. At low speeds ($M = 0.35$) the C_{D_F} of body 2, nose 2-A was about 7 percent greater than that of body 2, nose 2 (fig. 7). At higher speeds ($M = 0.60$) the drag increase was 8.6 percent. A very slight compressibility effect is thus indicated. With cooling-air flow it is likely that this drag increment would be decreased.

If the preceding comparisons are to be based on the fixed-transition data, it is well to note that the difference in drag of body 1, nose 1 was increased 29 percent (see figs. 5 and 9) by fixing transition. This value is in good agreement with calculations. Similar increments were observed for the other streamline models.

The large drag increments could be expected because at these Reynolds numbers extensive laminar boundary layers exist. At higher Reynolds numbers corresponding to full-scale conditions, no very extensive laminar boundary layers are obtained. The noted drag increase indicates the magnitude of difference due to boundary-layer conditions and demonstrates the importance of fixed-transition results for application at full-scale conditions. Possible errors resulting from the selection of the locations

at which transition occurs and from the effect of the small degree of tunnel turbulence on the normal-transition location are small and are believed to be not in excess of a few percent of the body length. These results as well as other tests indicate, moreover, that for bodies of the type investigated the compressibility effects are not altered by fixing the transition location.

The procedure of fixing transition cannot at present be assumed to give results exactly corresponding to full-scale conditions but the method does indicate the probability of large errors in the extrapolation of model data to high Reynolds numbers.

Radial-engine cowling-fuselage combinations.- The use of cowling C, closed, in place of the nose increased the values of C_{D_F} for bodies 1 and 2 with nose 1 from 15 to 21 percent, depending on the speed and the body (figs. 6 and 7). This increase was about twice as great as the increase caused by the nose opening in nose 2-A. Throughout the speed range for these tests, cowling C, closed, had compressibility effects similar to those of the streamline bodies.

At low speeds the results obtained with cowling 7, closed, were about the same as those obtained for cowling C. Cowling 7, however, had a low critical speed (M_{cr}, approximately 0.56) and is therefore undesirable for use at high speeds.

With cowling 5, closed, the increase in drag over the streamline body was considerably greater than with cowlings C and 7, closed. At a low speed (M = 0.18) the value of C_{D_F} was increased approximately 50 percent and at any higher speed a sharp drag increase occurred (approximately 400 percent). This effect was also noted in an earlier investigation (reference 3) and was shown to be due to separation rather than to compressibility effects. When cowling 5 was tested with cooling air, the sharp increase due to separation was delayed to a higher speed (M = 0.35). The results for cowling 5 show, however, that this shape is very critical and a slight change in angle of attack produced the sharp rise in drag even at speeds below that for separation at $\alpha_F = 0^\circ$; cowling 5 has therefore definitely poor drag characteristics at any speed.

When cooling air was allowed to pass through cowlings

C and 7 with baffles to simulate the pressure drop for engine cooling, increases in C_{D_F} were observed (figs. 9 and 10). Cowling 7 caused 8 percent higher C_{D_F} than cowling C caused for Mach numbers below the critical for cowling 7. This result was somewhat lower than the difference indicated in reference 3, but the variation may be due to the difference in the amount of cooling air in the two tests.

L-542

Wing-fuselage interference compressibility effects.- In an investigation that includes the combined compressibility effects of two or more parts, the amount which each contributes to the total becomes important. The computed M_{cr} for body 3, nose 3 alone was 0.88; for body 1, nose 1, 0.86; and, for the wing tested, 0.67. These values were calculated from the theoretical peak pressure (references 3 and 4) according to the $1/\sqrt{1 - M^2}$ variation (reference 5). By the addition of the superstream velocities of the component parts, the maximum superstream velocities of the combinations were obtained. These values indicated critical Mach numbers for these two wing-fuselage combinations of 0.63 and 0.62, respectively. These calculations indicate that the magnitude of the compressibility effects shown in these tests is largely due to the velocities over the wing and would be considerably less for the bodies alone. Comparisons of the compressibility effects between body 1, nose 1 and body 3, nose 3 are, however, correct because the peak superstream velocities of these fuselages and of the wing coincide.

The foregoing section shows that the wing, with a superstream velocity of 0.292V as compared with 0.069V and 0.086V for the fuselages, would be the logical part to improve in any conventional airplane design to obtain smaller compressibility effects and higher critical speeds. A more suitable wing would have a smaller maximum local velocity. For example, if a wing with a maximum superstream velocity 0.2V were used with body 3, nose 3, the computed speed would be at an M of 0.68 which, when compared with the computed value of $M_{cr} = 0.63$ for the test wing with the same fuselage, represents a difference in critical speed of about 40 miles per hour at standard sea-level conditions. Similar gains are obtainable for the other streamline fuselages with a wing having a lower peak local velocity than the test wings. The fixed critical speeds of the radial-engine cowlings prevent any further gains for combinations of these shapes. Thus, cowling C, the best

of these types, has a critical speed at an M of 0.623 (reference 3); no increases in critical speeds can be obtained in this case by changing the wing or the wing-body juncture.

CONCLUDING REMARKS

Tests of three streamline bodies with a test wing gave effective fuselage-drag coefficients from 0.046 to 0.057 at speeds from 260 to 440 miles per hour. At high speeds, the relative drag of two of these fuselage-wing combinations, differing only in fineness ratio, was considerably changed by compressibility effects.

Relatively blunt noses on streamline bodies in conjunction with a wing produced little or no changes in the drag or the compressibility effects. A cooling-air intake opening in the blunt nose caused about 7 percent increase in the drag with no significant changes in the compressibility effects.

The best radial-engine cowling-fuselage combinations had, without cooling air, drags from 18 to 21 percent greater than the corresponding streamline fuselages, depending on the speed and the body.

The critical speeds of the combinations tested were, in general, determined by the wing-fuselage juncture. Calculations show that, by an improvement of this region for the streamline bodies, material gains in critical speed would be obtainable. Similar gains in critical speed cannot be expected in systems using a conventional radial-engine cowling because of the low critical speed of the cowling itself.

Langley Memorial Aeronautical Laboratory,
National Advisory Committee for Aeronautics,
Langley Field, Va., July 10, 1940.

L-542

L-5-42

REFERENCES

1. Becker, John V., and Leonard, Lloyd H.: High-Speed Tests of a Model Twin-Engine Low-Wing Transport Airplane. NACA Rep. No. 750, 1942.

2. Abbott, Ira H.: Fuselage-Drag Tests in the Variable-Density Wind Tunnel: Streamline Bodies of Revolution, Fineness Ratio of 5. NACA TN No. 614, 1937.

3. Robinson, Russell G., and Becker, John V.: High-Speed Tests of Conventional Radial-Engine Cowlings. NACA Rep. No. 745, 1942.

4. Delano, James B.: Pressure Distribution on the Fuselage of a Midwing Airplane Model at High Speeds. NACA TN No. 890, 1943.

5. Stack, John, Lindsey, W. F., and Littell, Robert E.: The Compressibility Burble and the Effect of Compressibility on Pressures and Forces Acting on an Airfoil. NACA Rep. No. 646, 1938.

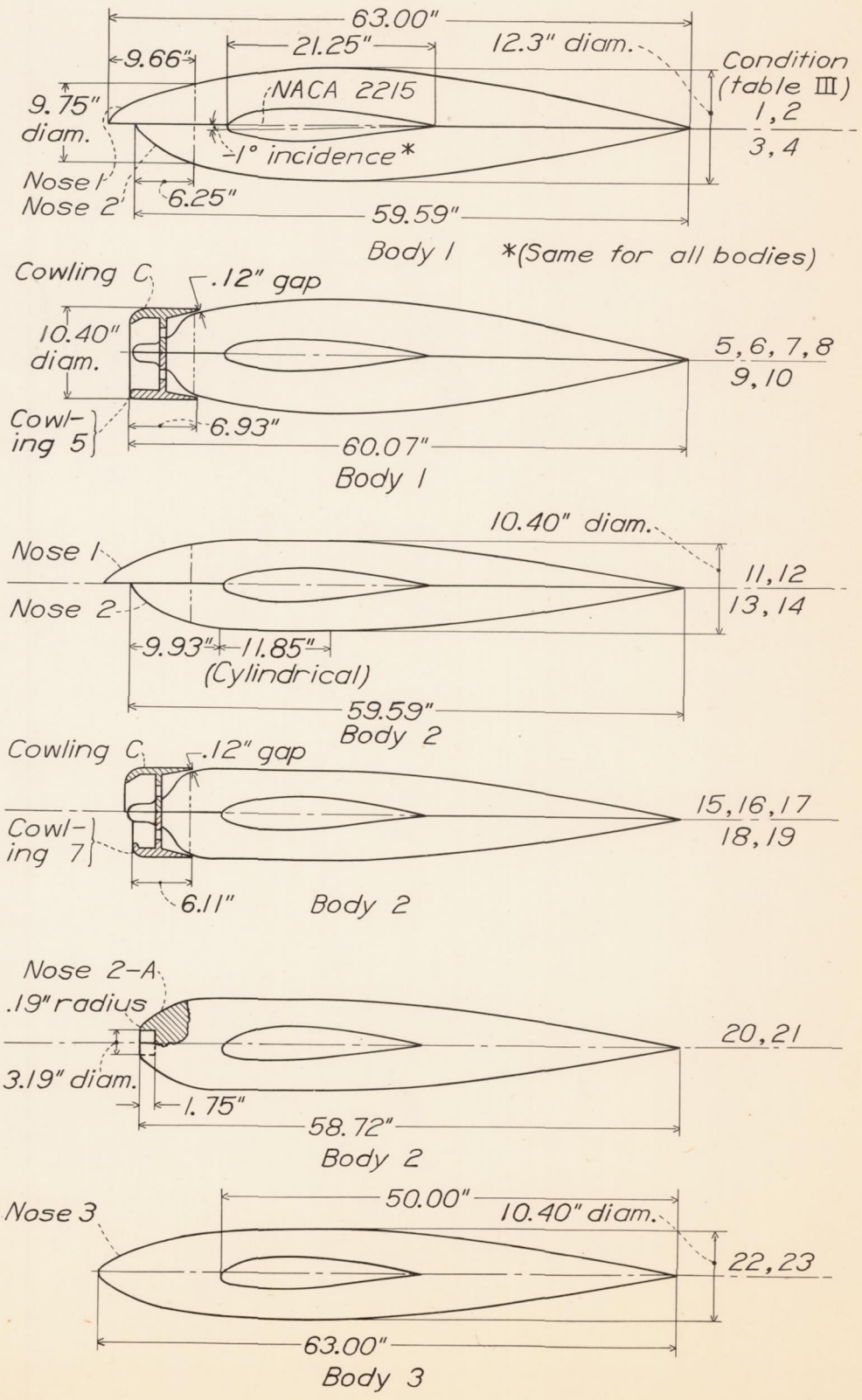


Figure 1.-Streamline shapes and cowling-fuselage combinations tested.

L-542

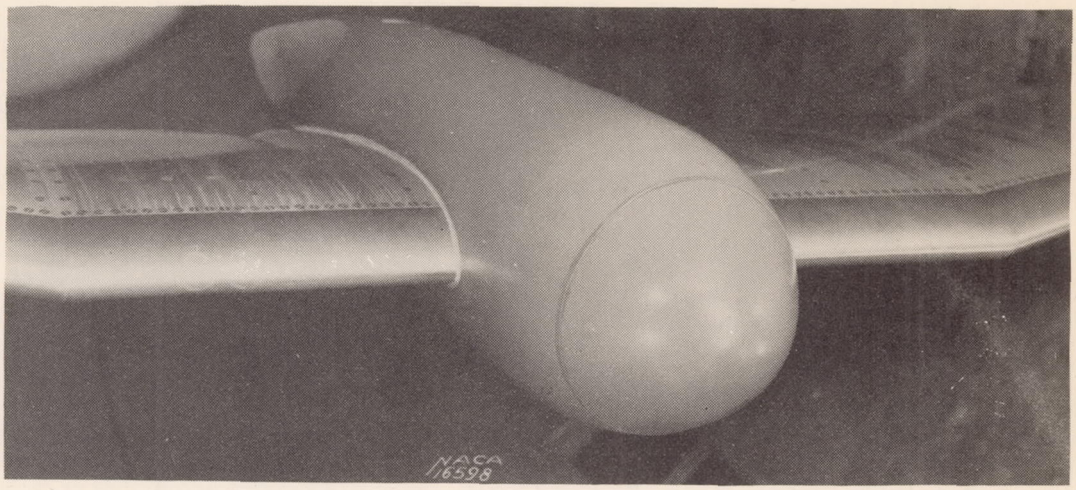


Figure 2.- Body 2, nose 2 with thread mounted on the test wing.

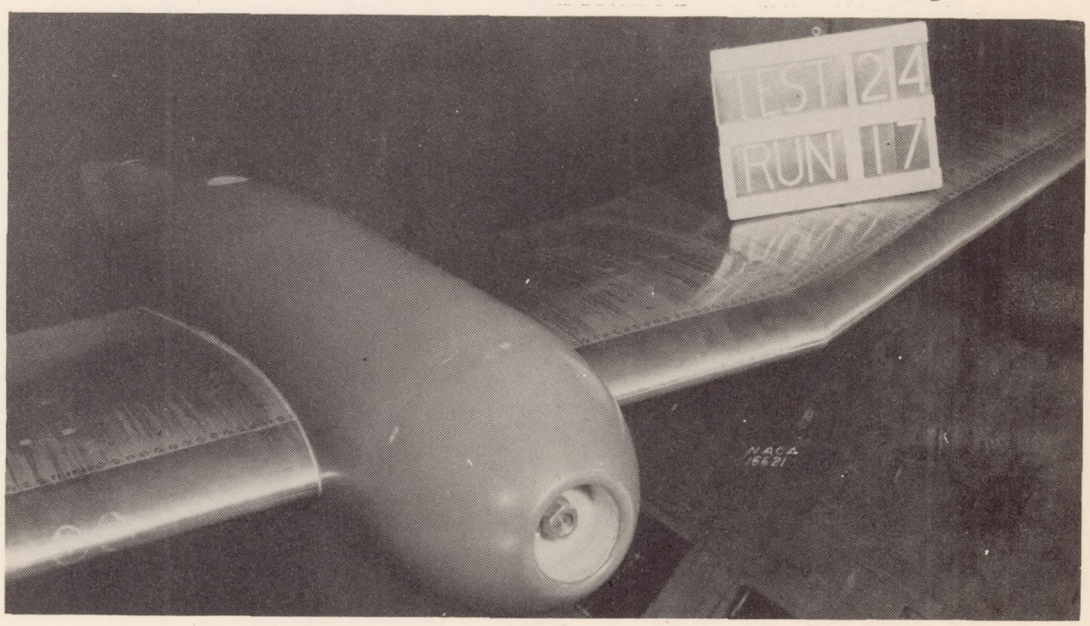


Figure 3.- Body 2, nose 2-A mounted on the test wing.

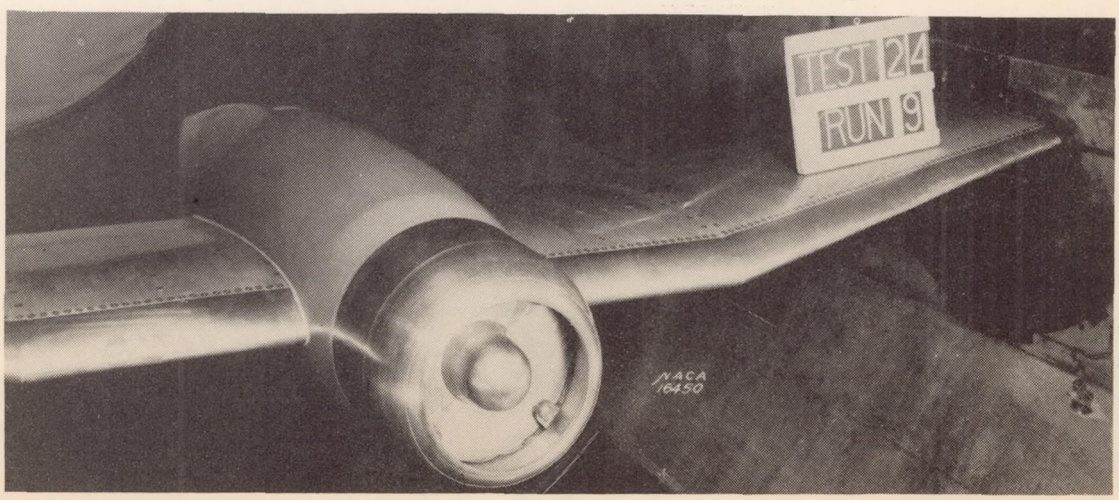


Figure 4.- Body 1, cowling C, closed with thread, mounted on the test wing.

L-542

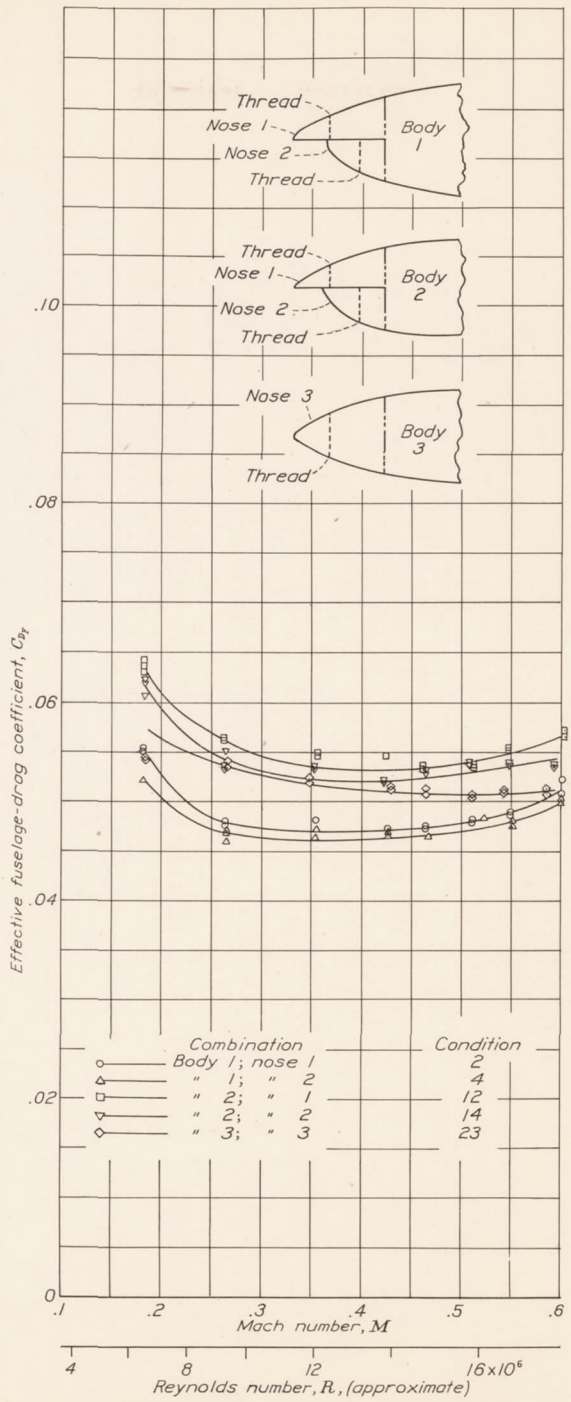


Figure 5.- Drag characteristics of streamline shapes with fixed transition; bodies 1, 2, and 3. α_F, 0°.

L-542

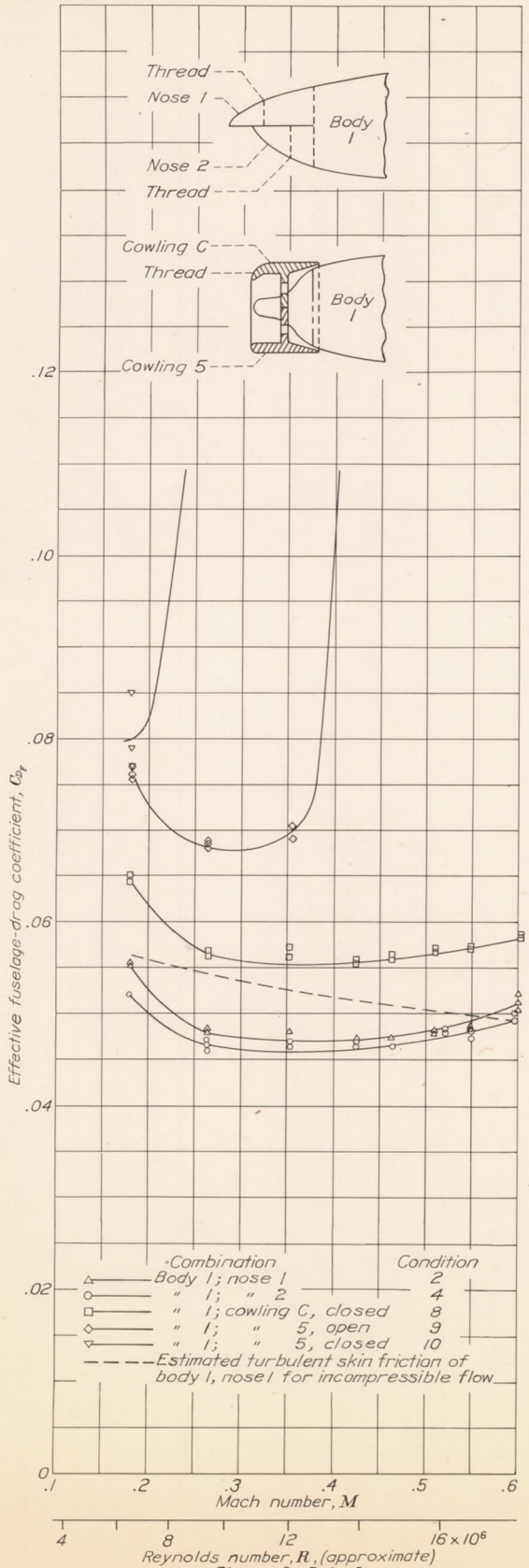


Figure 6. Body 1.

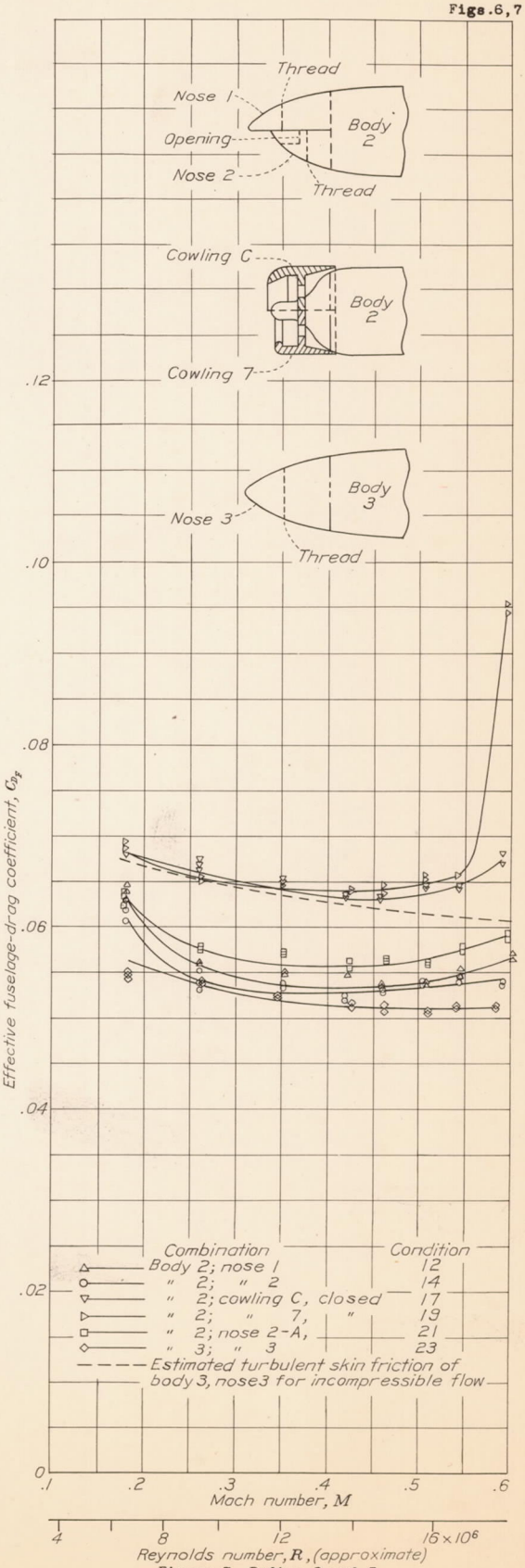


Figure 7. Bodies 2 and 3.

Figures 6,7.- Drag characteristics of cowlings and streamline noses with fixed transition; α_F , 0°.

L-542

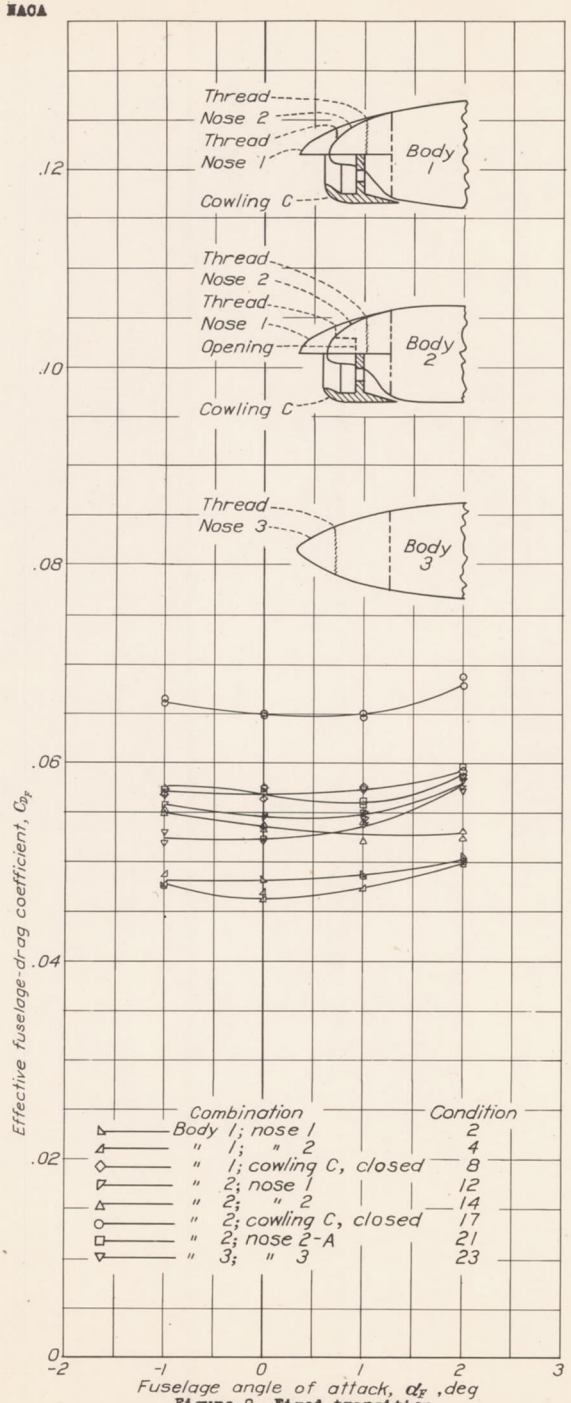


Figure 8.-Fixed transition.

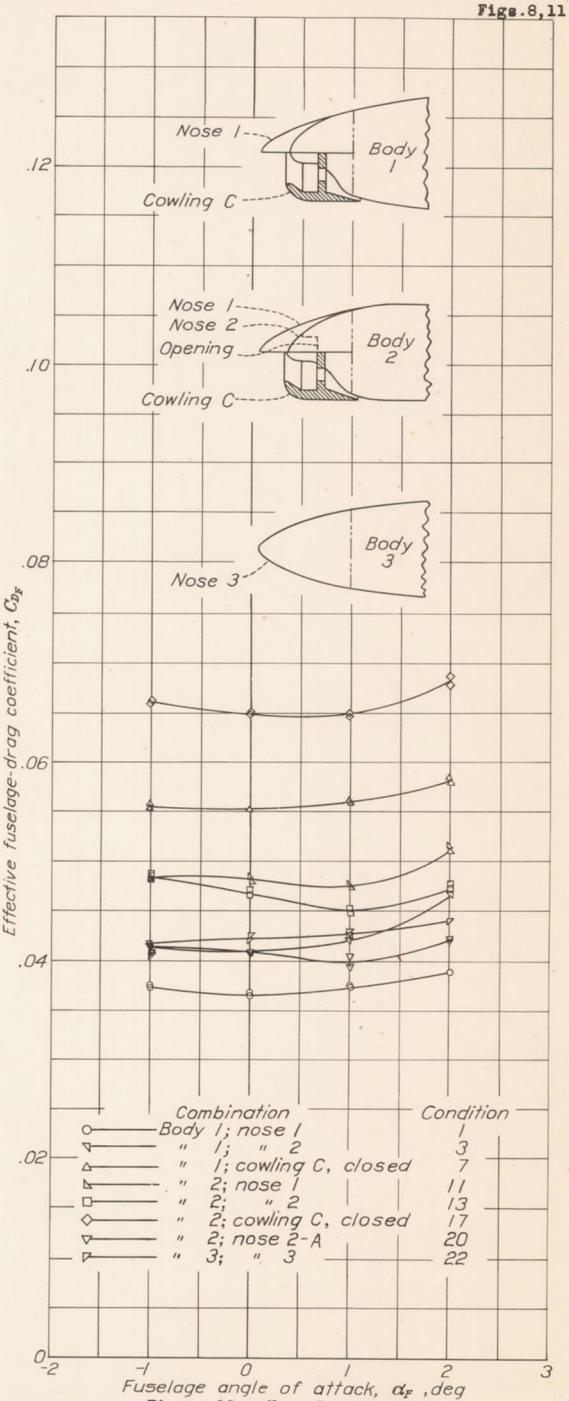


Figure 11.- Normal transition.

Figures 8,11.- Effect of angle of attack; M, approximately 0.35; R, approximately 3.5×10^6.

L-542

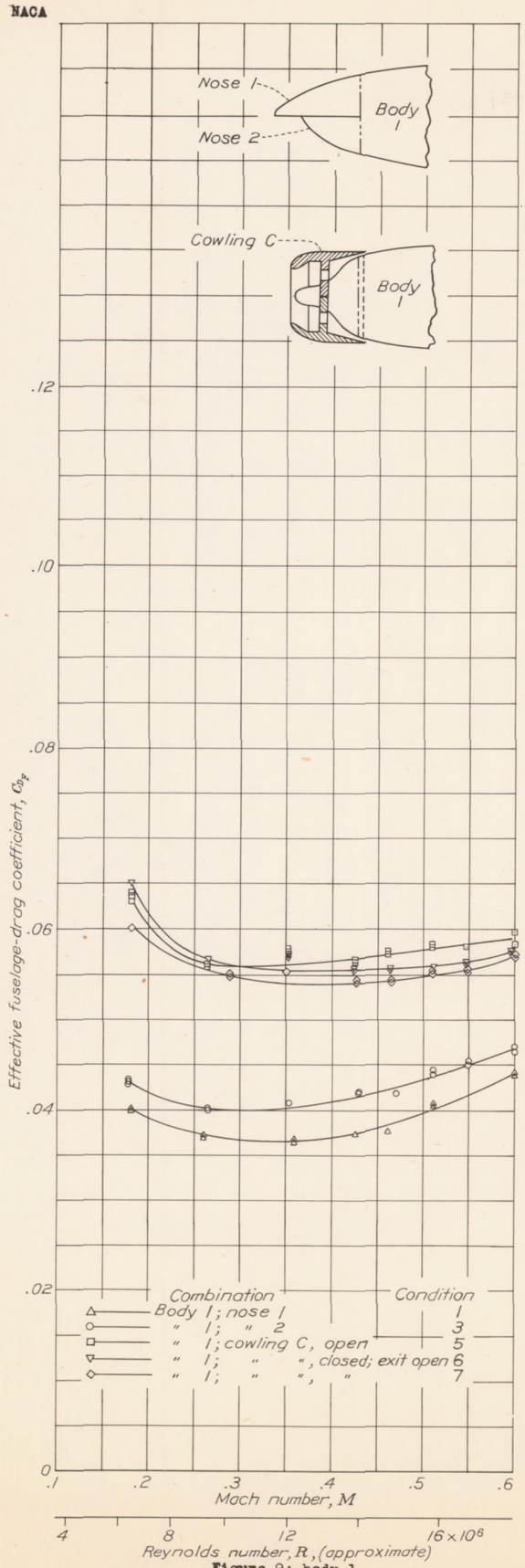


Figure 9; body 1.

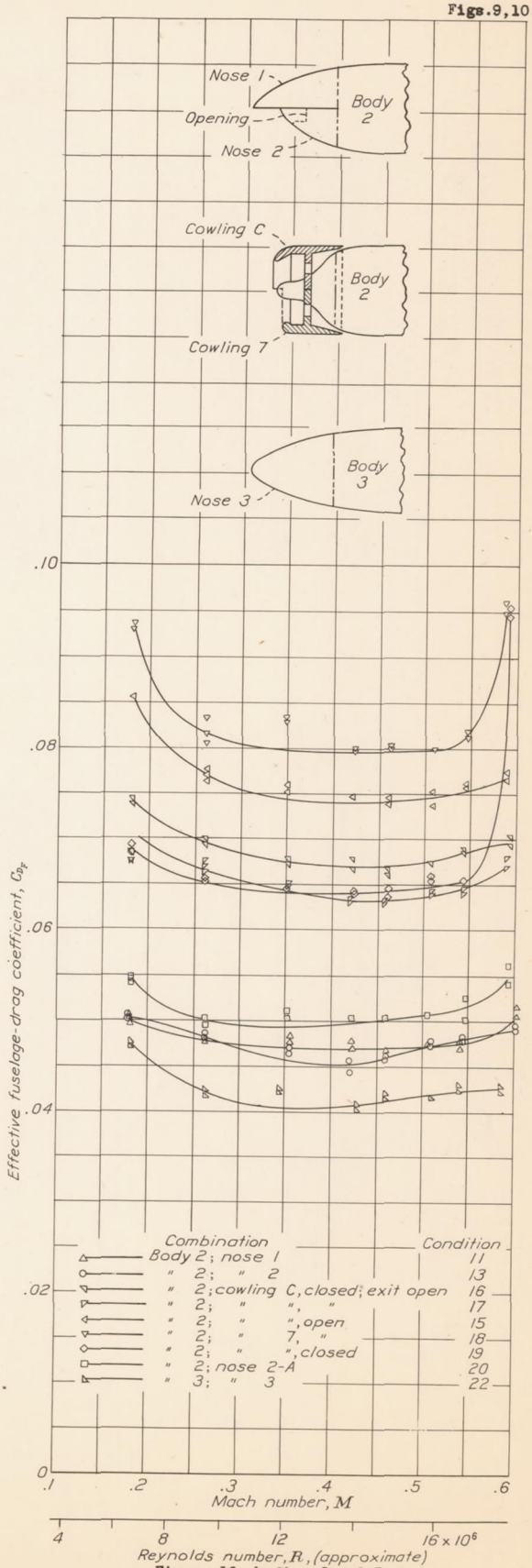


Figure 10; bodies 2 and 3.

Figures 9,10.- Drag characteristics of cowlings and streamline noses with normal transition; α_F, 0°.